

# Energetics and optical properties of 6-dimensional rotating black hole in pure Gauss-Bonnet gravity

Ahmadjon Abdujabbarov<sup>a,1,2</sup>, Farruh Atamurotov<sup>b,1,3</sup>, Naresh Dadhich<sup>c,4,5</sup>,  
Bobomurat Ahmedov<sup>d,1,2</sup>, Zdeněk Stuchlík<sup>e,6</sup>,

<sup>1</sup> Institute of Nuclear Physics, Ulughbek, Tashkent 100214, Uzbekistan

<sup>2</sup> Ulugh Beg Astronomical Institute, Astronomicheskaya 33, Tashkent 100052, Uzbekistan

<sup>3</sup> Inha University in Tashkent, Tashkent 100170, Uzbekistan

<sup>4</sup> Inter-University Centre for Astronomy and Astrophysics, Post Bag 4, Ganeshkhind, Pune 411 007, India

<sup>5</sup> Centre for Theoretical Physics, Jamia Millia Islamia, New Delhi 110025, India

<sup>6</sup> Institute of Physics, Faculty of Philosophy and Science, Silesian University in Opava, Bezrucovo nam. 13, Opava, Czech Republic

the date of receipt and acceptance should be inserted later

**Abstract** We study physical processes around a rotating black hole in pure Gauss-Bonnet (GB) gravity. In pure GB gravity, gravitational potential has slower fall off as compared to the corresponding Einstein potential in the same dimension. It is therefore expected that the energetics of pure GB black hole would be weaker, and our analysis bears out that the efficiency of energy extraction by Penrose process is increased to 25.8% and particle acceleration is increased to 55.28%, and optical shadow of the black hole is decreased. These are the distinguishing in principle observable features of pure GB black hole.

## 1 Introduction

From all the generalizations of Einstein gravity what distinguishes the Lovelock gravity is its remarkable property that the equation of motion always remains second order. This happens despite the Lagrangian being polynomial in Riemann curvature. It is the underlying differential geometric structure that is responsible for this unique remarkable property, discovered by Lovelock [1]. Lovelock action  $S$  which is a homogeneous polynomial of degree  $N$  in Riemann curvature reads as

$$S = \int \sqrt{-g} \left( \sum_N \lambda_N \mathcal{L}_N \right) d^D x, \quad (1)$$

where the Lagrangian is given by

$$\mathcal{L}_N = \frac{1}{2^N} \delta^{\alpha_1 \dots \alpha_N \beta_1 \dots \beta_N}_{\gamma_1 \dots \gamma_N \mu_1 \dots \mu_N} R^{\gamma_1 \mu_1}_{\alpha_1 \beta_1} \dots R^{\gamma_N \mu_N}_{\alpha_N \beta_N}, \quad (2)$$

<sup>a</sup> e-mail: ahmadjon@astrin.uz

<sup>b</sup> e-mail: farruh@astrin.uz

<sup>c</sup> e-mail: nkd@iucaa.ernet.in

<sup>d</sup> e-mail: ahmedov@astrin.uz

<sup>e</sup> e-mail: zdenek.stuchlik@fpf.slu.cz

and  $\lambda_N$  are coupling constants. In this action  $N = 0, 1, 2, \dots$  respectively correspond to  $\Lambda$ , the usual Einstein-Hilbert, Gauss-Bonnet and so on. However higher order Lovelock terms in action make non-zero contribution only in dimensions  $> 4$ . That is Lovelock is the natural higher dimensional generalization of Einstein gravity.

It is well-known that particle physics theories, in particular string theory, call for higher dimensions as demanded by physical symmetries. Besides one of us had also articulated some purely classical considerations for higher dimensions [2, 3, 4]. One of the most convincing arguments goes as follows [4]. It is customary to consider high energy effects of a theory by taking higher power of the basic variable. In the case of gravity, the basic physical entity is Riemann curvature and hence to take into account high energy effects, we should include higher powers of it in the action. However if we demand that the equation of motion should not change its second order character, then we are uniquely led to Lovelock action which is pertinent only in higher dimensions. That is high energy effects of gravity are accessible only in higher dimensions. Thus it makes a good case for studying gravity in higher dimensions.

Note that in the above action, there is sum over  $N$  and each term has a dimensionful coupling constant which cannot be determined because experiment can determine only one constant. To make problem tractable, it was assumed, for obtaining dimensionally continued black holes [5], that all the couplings were given in terms of the unique ground state  $\Lambda$ . On the other hand, there is a strong case made out for pure Lovelock gravity [6, 7] where there is only one  $N$ th order term in

the action with  $A$ . That is, it does not include even the usual Einstein-Hilbert term. This has remarkable unique property that gravitational dynamics is distinguished in all odd and even dimensions [7]. In all odd  $D = 2N + 1$  dimensions, gravity is kinematic meaning  $N$ th order Lovelock analogue Riemann tensor vanishes whenever the corresponding Ricci tensor vanishes [8]. This of course includes the usual 3 dimension for which Riemann tensor is entirely given in terms of Ricci tensor showing kinematic property of Einstein gravity for  $N = 1$ . It is thus a universal feature of pure Lovelock gravity. We will therefore adhere to pure Lovelock generalization for exploring gravity in higher dimensions.

Rotating black holes are by far the most exciting objects as they offer a rich arena of interesting physical processes of astrophysical importance in the usual four spacetime dimensions. These include high energy exotic objects like quasars and active galactic nuclei (AGNs) with their energetic jets, energy extraction processes by Penrose process [9] and its magnetic version [10, 11, 12, 13, 14, 15] and Blandford-Znajek mechanism [16] and particle acceleration [17] as well as optical shadow of black hole, see, e.g., [18, 19, 20, 21, 22, 23, 24]. The possibility to obtain ultra-high energy particles and the appearance of Keplerian discs orbiting Kerr superspinars have been studied in [25, 26]. Keeping in view physical richness and astrophysical significance of rotating black holes, it would be pertinent to probe these interesting properties for higher dimensional rotating black holes. As argued above, in higher dimensions, pure Lovelock gravity enjoys an unique special position in view of its universal characteristics for all odd and even dimensions. It would therefore be pertinent to study interesting physical and astrophysical phenomena for a pure GB rotating black hole in six dimension. Apart from astrophysical motivation for this study, there is a fundamental question of what shape gravitational dynamics takes in higher dimensions? For instance in Einstein gravity, gravitational field becomes stronger as dimension increases which implies that there can exist no bound orbits in dimension greater than four while for pure Lovelock gravity, it becomes weaker with dimension and hence bound orbits continue to exist in all even dimensions [27].

Very recently, a rotating black hole metric has been obtained [28] to describe an analogue of Kerr black hole in pure GB gravity in six dimensions. Though it is not an exact solution of the pure Lovelock vacuum equation, it has all the desirable and expected features and it satisfies the equation in the leading order. In this paper, we wish to study energetics of pure GB rotating

black hole by employing this metric. Our study yields results which are in tune with the general properties of a rotating black hole and hence it further lends support to the metric for its viability.

Note that Einstein gravity is vacuum in two, kinematic in three and becomes dynamic in four dimensions, and it is pure Lovelock of order  $N = 1$ . The universalization of this general gravitational feature means gravity should respectively be vacuum, kinematic and dynamic for  $D = 2N, 2N + 1, 2N + 2$ . This uniquely picks out pure Lovelock gravity; i.e. pure Lovelock should be the gravitational equation in higher dimensions. That is in all odd and even  $D = 2N + 1, 2N + 2$  dimensions gravitational dynamics should be similar [29]. This is what has been verified in various situations; for instance black hole entropy is always proportional to square of horizon radius [6, 7] and bound orbits around static black hole exist only for the pure Lovelock gravity in all even  $D = 2N + 2$  dimensions [27]. This motivates us to examine this general feature in all possible situations and that is what we wish to do in this paper. We shall therefore study all the usual physical processes like energy extraction, Hawking radiation, optical shadow and particle acceleration for a pure GB rotating black hole [28] and compare them to that of a rotating black hole in the usual four dimensional spacetime. This is the primary aim of the paper.

The paper is arranged as follows: the rotating black hole metric is discussed in Sec. 2 while in Sec. 3, we analyze the geodesic equations for circular orbits which is followed by discussion of optical shadow of black hole in Sec. 4. Next we study energy extraction processes through BSW effect and Penrose process. We conclude with a discussion. Throughout the paper, we use a system of units in which the GB coupling constant and velocity of light are set to unity.

## 2 Pure GB rotating black hole metric

We wish to consider a pure Gauss-Bonnet rotating black hole in the critical 6 dimension (in odd  $d = 5$  GB gravity is kinematic; i.e. GB flat and it becomes dynamic in even  $d = 6$  [7]). There does not exist an exact solution of pure GB vacuum equation for an axially symmetric spacetime representing a rotating black hole. This is simply because the equations are very formidable to handle. However for Einstein gravity in 4 dimension there is the well known Newman-Janis algorithm for converting a static black hole into a rotating one without solving the equation. This may however not be applicable for GB gravity and in higher dimension [30].

Secondly one of us [31] has recently obtained the Kerr metric by appealing to the two simple physical considerations. One, it should incorporate Newton's law in the first approximation, and second, since one is free to choose affine parameter for a null curve and hence the radial coordinate is chosen as affine parameter for radially falling photon. For this, one begins with an appropriate spatial geometry which has ellipsoidal symmetry and then implement these two common sense inspired physical considerations, and what results is the metric [28] considered here. This can describe a rotating black hole, though it is not an exact solution of pure GB vacuum equation, yet it has all the features of the usual Kerr metric. It however does satisfy the equation in the leading order. It has all the characteristics of a rotating black hole in existence of ergosphere, and the right limits; for  $a = 0$  it reduces to pure GB static black hole while  $M = 0$  leads to flat space. It is therefore perfectly appropriate metric for studying a rotating black hole in pure GB gravity. We shall thus employ this rotating black hole metric for studying its various physical properties.

The stationary axisymmetric metric for pure GB rotating black hole in the standard Boyer-Lindquist coordinates reads as [28]

$$ds^2 = -\frac{\Delta}{\Sigma} \left[ dt - a^2 \sin^2 \theta d\phi \right]^2 + \frac{\Sigma}{\Delta} dr^2 + \Sigma d\theta^2 + \frac{\sin^2 \theta}{\Sigma} \left[ (r^2 + a^2) d\phi - a dt \right]^2 + r^2 \cos^2 \theta [d\psi^2 + \sin^2 \psi d\chi^2], \quad (3)$$

with

$$\Delta = r^2 + a^2 - M^{1/2} r^{3/2}, \quad \Sigma = r^2 + a^2 \cos^2 \theta, \quad (4)$$

where  $M$  and  $a$  have usual meaning of the total mass and specific angular momentum.

The spacetime (3) has horizon when  $t = \text{const}$  becomes null; i.e.  $\Delta = 0$  which has the following four roots

$$r_{+,-} = \frac{M}{4} + \frac{C}{4\sqrt{3}} \pm \sqrt{\frac{3M^2}{16} - a^2 - \frac{C^2}{192} + \sqrt{3} \frac{M^3 - 8a^2M}{8C}}, \quad (5)$$

$$r_{3,4} = \frac{M}{4} - \frac{C}{4\sqrt{3}} \pm \sqrt{\frac{3M^2}{16} - a^2 - \frac{C^2}{192} - \sqrt{3} \frac{M^3 - 8a^2M}{8C}}, \quad (6)$$

with

$$C^2 = 3M^2 - 16a^2 + \frac{64a^4}{A} + 4A, \quad A^3 = \frac{27}{2} a^4 M^2 - 64a^6 + 3\sqrt{3} a^4 M D, \quad D = \sqrt{\frac{27}{4} M^2 - 64a^2}.$$

The function under the square root in expression (6)

$$F_1(a, M) = \frac{3M^2}{16} - a^2 - \frac{C^2}{192} - \sqrt{3} \frac{M^3 - 8a^2M}{8C}$$

is always negative and consequently  $r_{3,4}$  is not real, while the function under the square root in expression (5)

$$F_2(a, M) = \frac{3M^2}{16} - a^2 - \frac{C^2}{192} + \sqrt{3} \frac{M^3 - 8a^2M}{8C}$$

is non-negative for the range of rotation parameter  $|a| \leq 3\sqrt{3}M/16$  (see Fig. 4), the equality indicates the extremal value of the rotation parameter. It is  $r_{+,-}$  that mark outer and inner horizons of the hole. The static limit is defined where the time-translation Killing vector  $\xi_{(t)}^\alpha$  becomes null (i.e.  $g_{00} = \Delta - a^2 \sin^2 \theta = 0$ ). The region bounded by the outer horizon and the static limit defines the ergosphere (See Fig. 1), the extent of which increases with the rotation  $a$  of the hole.

### 3 Geodesics and circular orbits

In order to study particle motion around six dimensional pure GB black hole we first write the Hamilton-Jacobi equation,

$$\frac{\partial S}{\partial \sigma} = -\frac{1}{2} g^{\mu\nu} \frac{\partial S}{\partial x^\mu} \frac{\partial S}{\partial x^\nu}, \quad (7)$$

for Hamiltonian [32, 33, 34]:

$$S = \frac{1}{2} m^2 \sigma - \mathcal{E} t + \mathcal{L} \phi + S_r(r) + S_\theta(\theta) + \mathcal{W} \chi + T_\psi(\Psi), \quad (8)$$

where  $m$  is mass,  $\mathcal{E}$  and  $\mathcal{L}$  are conserved energy and angular momentum of the particle.

The issue of the separability of the Hamilton-Jacobi equation in higher dimensional spacetime has been widely studied in the literature [32, 33, 34]. Particularly, the authors of the paper [32, 33] have shown that the spacetime metric (3) is Petrov type D.

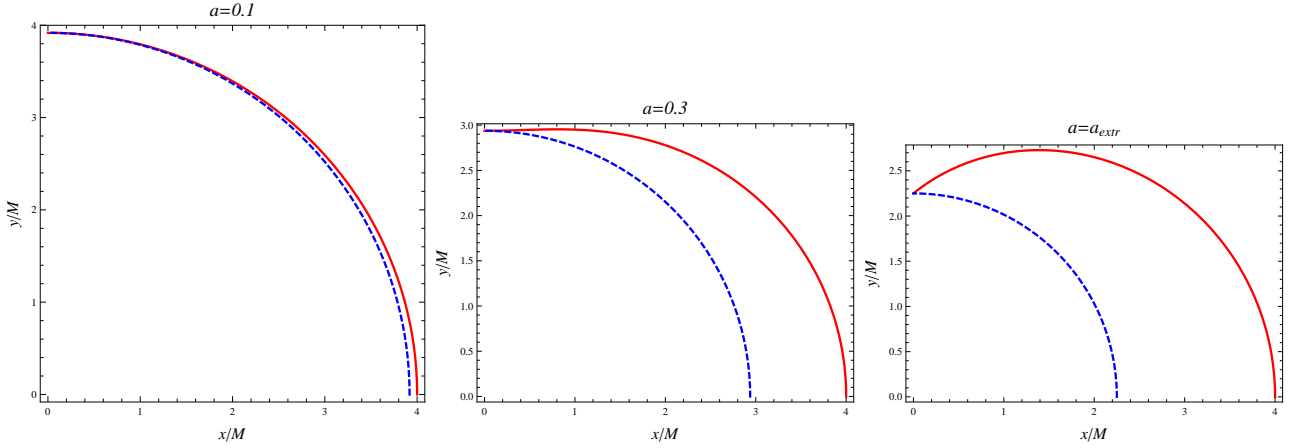


**Fig. 1** The ergosphere for the different values of the spin parameter  $a$ :  $a/M = 0.1$  (left panel),  $a/M = 0.3$  (middle panel), and  $a/M = a_{extr}/M = 3\sqrt{3}/16$  (right panel). Red lines indicate static limit while dashed blue lines indicate horizon.

### 3.1 Null circular orbits

For null geodesics (when  $m = 0$ ), one can get the equations of motion from the Hamilton-Jacobi equation (7) as

$$\begin{aligned} \Sigma \frac{dt}{d\sigma} &= a(\mathcal{L} - a\mathcal{E} \sin^2 \theta) + \frac{r^2 + a^2}{\Delta} [(r^2 + a^2)\mathcal{E} - a\mathcal{L}] \quad (9) \\ \Sigma \frac{d\phi}{d\sigma} &= \left( \frac{\mathcal{L}}{\sin^2 \theta} - a\mathcal{E} \right) + \frac{a}{\Delta} [(r^2 + a^2)\mathcal{E} - a\mathcal{L}] \quad (10) \\ \cos^2 \theta \frac{d\chi}{d\sigma} &= \frac{\csc^2 \psi}{r^2} \mathcal{W} \quad (11) \\ \Sigma \frac{dr}{d\sigma} &= \sqrt{\mathcal{R}} \quad (12) \\ \Sigma \frac{d\theta}{d\sigma} &= \sqrt{\Theta} \quad (13) \\ \cos^2 \theta \frac{d\psi}{d\sigma} &= \frac{\mathcal{W}}{r^2 \sin \psi} \quad (14) \end{aligned}$$

where new functions  $\mathcal{R}(r)$  and  $\Theta(\theta)$

$$\mathcal{R} = [(r^2 + a^2)\mathcal{E} - a\mathcal{L}]^2 - \Delta[\mathcal{K} + (\mathcal{L} - a\mathcal{E})^2] \quad (15)$$

$$\Theta = \mathcal{K} - \frac{1}{\sin^2 \theta} [a\mathcal{E} \sin^2 \theta - \mathcal{L}]^2 \quad (16)$$

are introduced.

The conserved quantity  $\mathcal{W}$  exists only when  $\theta \neq \pi/2$  and is similar to angular momentum. So called Carter constant  $\mathcal{K}$  characterizes together with the quantities  $\mathcal{E}$ ,  $\mathcal{W}$  and  $\mathcal{L}$  the geodesic motion. The Carter constant is not related to any isometry of the space-time unlike the conserved quantities  $\mathcal{E}$ ,  $\mathcal{W}$  and  $\mathcal{L}$ .

By defining  $\xi = \mathcal{L}/\mathcal{E}$ ,  $\eta = \mathcal{K}/\mathcal{E}^2$  and  $\zeta = \mathcal{W}/\mathcal{E}$  and using Eq. (12) we get for the circular orbits characterized by  $\mathcal{R}(r) = 0$  and  $d\mathcal{R}(r)/dr = 0$ ,

$$\xi(r, a) = \frac{a^2(2r + 3r^{1/2}) + r^2(2r - 5r^{1/2})}{a(3r^{1/2} - 2r)} \quad (17)$$

$$\eta(r, a) = \frac{8a^2 r^{7/2} - r^4(2r - 5r^{1/2})^2}{a^2(2r - 3r^{1/2})^2} \quad (18)$$

### 3.2 Timelike circular orbits

Consider the equation of motion of test particle with nonzero rest mass at the equatorial plane ( $\theta = \pi/2$ ,  $\dot{\theta} = 0$ ). The equations of motion take the following form

$$m \frac{dt}{d\sigma} = - \frac{\mathcal{E}r^2 - a\mathcal{L}\sqrt{M/r} + a^2 E (\sqrt{M/r} + 1)}{a^2 - M^{1/2}r^{3/2} + r^2} \quad (19)$$

$$m \frac{d\phi}{d\sigma} = \frac{\mathcal{L} + (a\mathcal{E} - \mathcal{L})M^{1/2}r^{-1/2}}{a^2 - M^{1/2}r^{3/2} + r^2} \quad (20)$$

$$m^2 \left( \frac{dr}{d\sigma} \right)^2 = \mathcal{E}^2 - V_{\text{eff}} \quad (21)$$

(13) where

$$\begin{aligned} (14) \quad V_{\text{eff}} &= m^2 \left( 1 - \sqrt{\frac{M}{r}} \right) - \frac{(\mathcal{L} - a\mathcal{E})^2 M^{1/2}}{r^{5/2}} \\ &+ \frac{\mathcal{L}^2 - a^2(\mathcal{E}^2 - m^2)}{r^2} \quad (22) \end{aligned}$$

is the effective potential for radial motion. Note that for the orbits in the equatorial plane the new conserved quantity  $\mathcal{W}$  does not appear in the equations of motion. In Fig. 2 the radial dependence of the effective potential of radial motion in equatorial plane has been shown for the fixed specific value of the rotation parameter  $a = M$ . The increase of the momentum of the particle leads to the increase of the peak of the potential: initially infalling test particles become bounded or escaped with the increase of the momenta.

The conditions of occurrence of circular orbits are

$$\frac{dr}{d\sigma} = 0, \quad V'_{\text{eff}}(r) = 0.$$

From these equations, it follows that energy  $\mathcal{E}$  and angular momentum  $\mathcal{L}$  of a circular orbit of radius  $r_c$  are

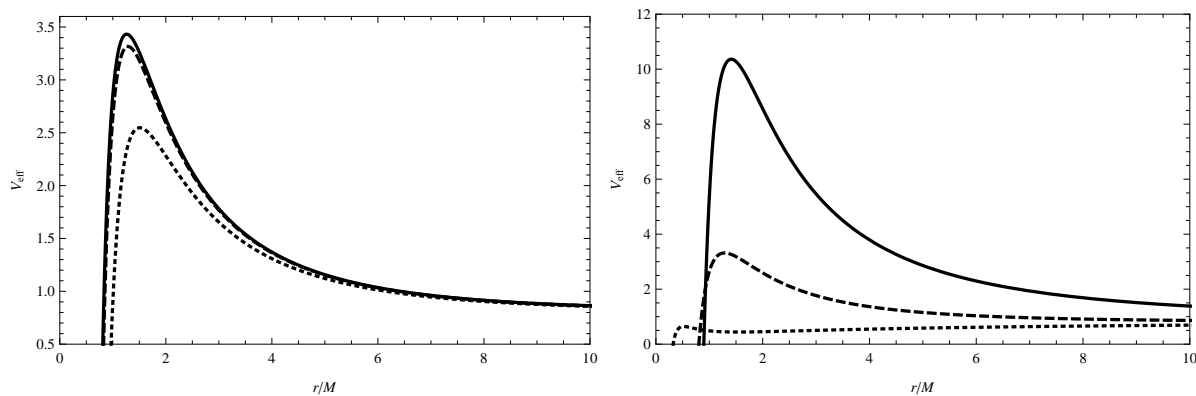


**Fig. 2** The radial dependence of effective potential for the different values of angular momentum and rotation parameter. The left plot corresponds to the case when  $a$  varies and the graphs are plotted for the different values of rotation parameter:  $a/M = 0.1$  (dotted line),  $a/M = 0.3$  (dashed line), and  $a/M = a_{extr}/M = 3\sqrt{3}/16$  (solid line). The right plot corresponds to the case when  $L$  varies and the graphs are plotted for the different values of the angular momentum of the particle:  $L/Mm = 1$  (dotted line),  $L/Mm = 5$  (dashed line), and  $L/Mm = 10$  (solid line)

given by

$$\mathcal{E}^2 = \left[ a^2(12\sqrt{r} - 11)r^2 - 4(\sqrt{r} - 1)^2(4\sqrt{r} - 5)r^{7/2} \pm 4ar^{5/4}(a^2 - r^{3/2} + r^2) \right] \times \left[ 16a^2r^{5/2} - (5 - 4\sqrt{r})^2r^4 \right], \quad (23)$$

$$\mathcal{L}^2 = \left[ 5r^6 - a^4(11 + 4\sqrt{r})r^2 - 4r^{13/2} + 2a^2(10 - 11\sqrt{r} - 4r)r^{7/2} \pm (a^2 - r^{3/2} + r^2)(20r^2 + 4a^2) \right] \times \left[ 16a^2r^{5/2} - (5 - 4\sqrt{r})^2r^4 \right]^{-1}, \quad (24)$$

where  $+$  and  $-$  signs correspond to the co-rotating and counter-rotating particles.

In the Fig. 3 we have shown energy and angular momentum of the co and counter rotating orbits in the equatorial plane for different values of rotation parameter  $a$ . One can easily see the shift in location of the minimal circular orbit (MC) marking the existence limit given by the photon circular orbit and the innermost stable circular orbits (ISCO). The MC and ISCO come closer to the hole with increase in  $a$  for co-rotating orbits while opposite happens for counter rotating ones.

The vanishing of denominator in the expressions for  $\mathcal{E}$  and  $\mathcal{L}$  marks the location of photon circular orbit or MC while for ISCO we have  $dr/d\sigma = V'_{\text{eff}}(r) = 0$  and  $V''_{\text{eff}}(r) \geq 0$ . In Fig. 4 we have shown three regions as dark, light grey and white marking the boundaries of stable, unstable and no circular orbits. The inner boundary of light grey is defined by photon circular orbit and the white region bounded between it

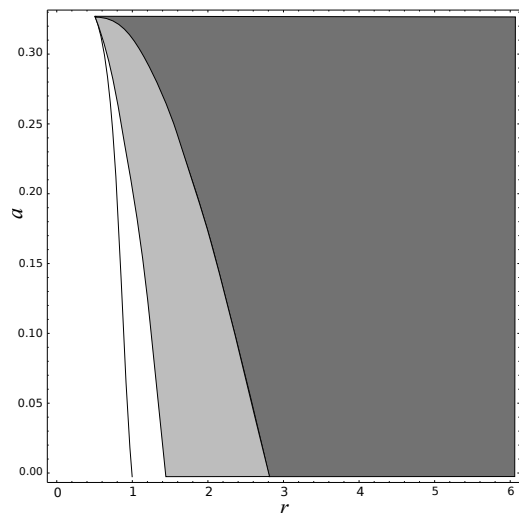


**Fig. 4** The regions of stable (dark grey) and unstable (light grey) circular orbits. The black curve indicates the border of event horizon of 6-D Gauss-Bonnet black hole.

and the horizon is the one where no circular orbits can exist. This is the region between  $3M$  and  $2M$  for the Schwarzschild black hole. As expected these regions are quite similar to that of the 4-dimensional Kerr black hole.

At this point it may be mentioned that bound orbits cannot exist for Einstein gravity in dimensions  $\geq 4$  [7] in general and in particular their non-existence is shown for 6-dimensional rotating black hole in Ref. [35]. For pure Lovelock gravity they do always exist in all even dimensions,  $d = 2N + 2$  [7].

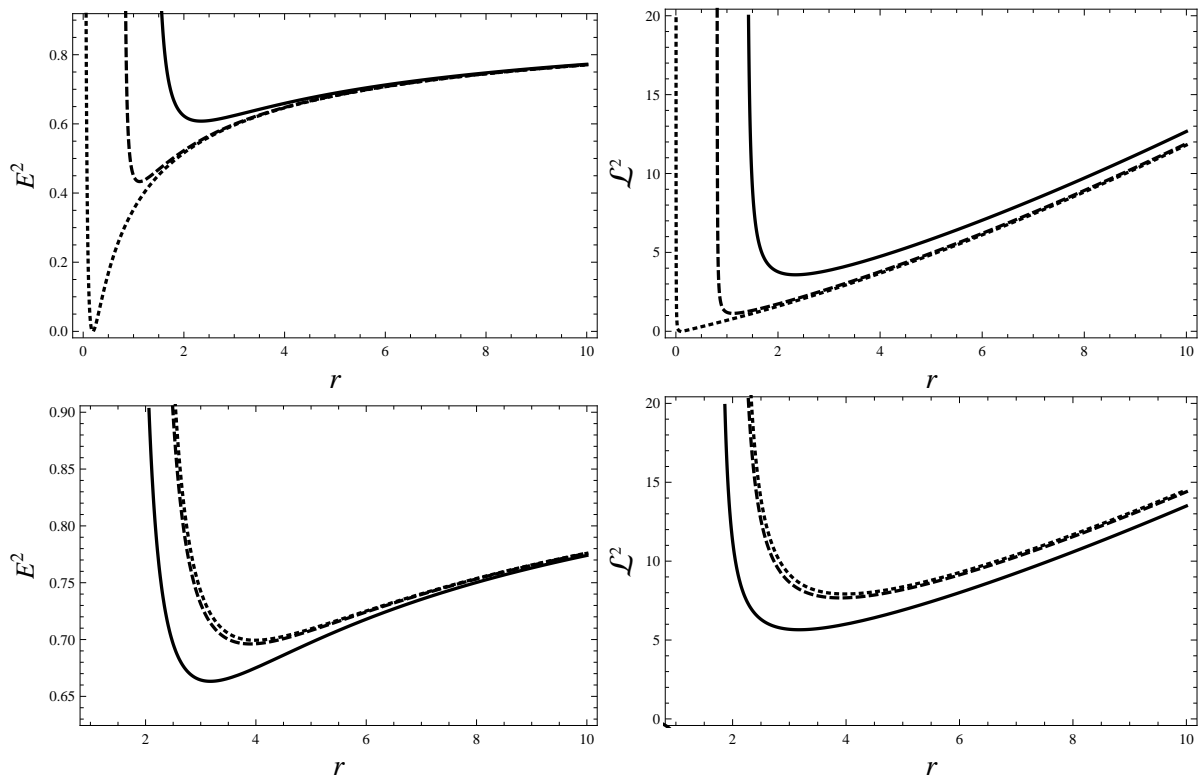


**Fig. 3** The radial dependence of energy (left) and angular momentum (right) squared of counter-rotating (upper plots) and co-rotating (lower plots) particle at circular orbits for the different values of parameter  $a = 0.1$  (solid line),  $0.3$  (dashed line), and  $3\sqrt{3}/16$  (dotted line).

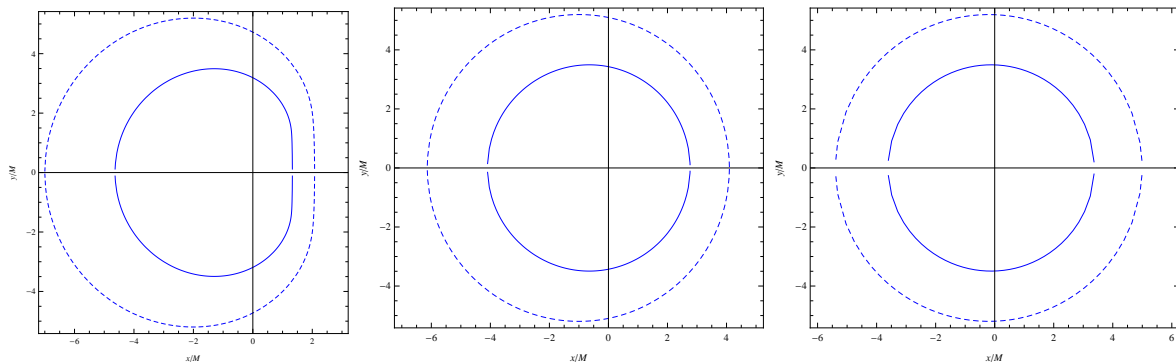


**Fig. 5** Shadow of the rotating GB black holes when the inclination angle  $\theta = \pi/2$ . For the comparison we present the shadow of rotating Kerr black hole (dashed lines). From left to right, the rotation parameter scans as  $a = 0$ ,  $a_{\text{ext}}/2$ , and  $a_{\text{ext}}$ . Note that for the pure GB 6-D black hole  $a_{\text{ext}} = 3\sqrt{3}/16$  as against  $a_{\text{ext}} = 1$  for the Kerr black hole.

#### 4 Black hole shadow

In this section we study the optical properties of black hole in Gauss-Bonnet gravity. If the bright source is located behind black hole then a distant observer is able to detect only photons scattered away from the black hole, and those captured by the event horizon form a dark spot. This dark region which could be detected and extracted from the luminous background is traditionally called the black hole shadow or silhouette. In

practice, the distant observer at infinity could see a projection of it at the flat plane passing through the black hole and normal to the line connecting it with the observer (the line of sight). The Cartesian coordinates at this plane, which are usually denoted by  $\alpha$  and  $\beta$  and called celestial coordinates, give the apparent position of the shadow image. The celestial coordinates are connected with the geodesic equations of photons around

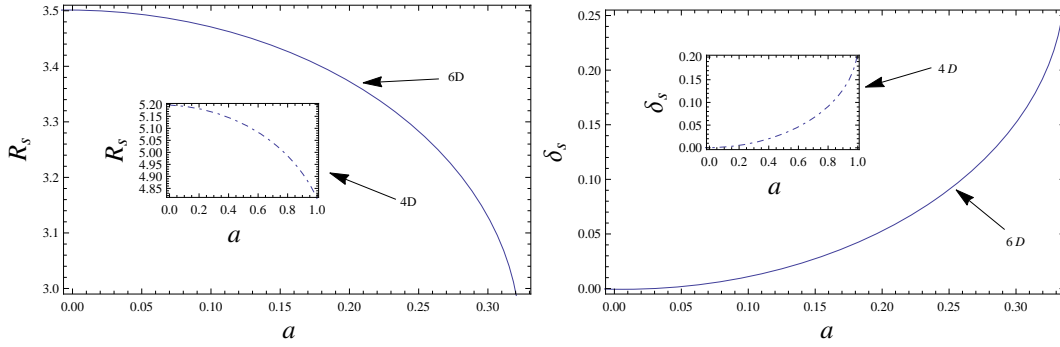


**Fig. 6** Observables  $R_s$  and  $\delta_s$  as functions of the rotation parameter, corresponding to the shadow of black hole situated at the origin of coordinates with inclination angle  $\theta = \pi/2$  and dimensions  $d$ :  $D = 6$  (solid line) and  $d = 4$  (dot-dashed line) [36, 37].

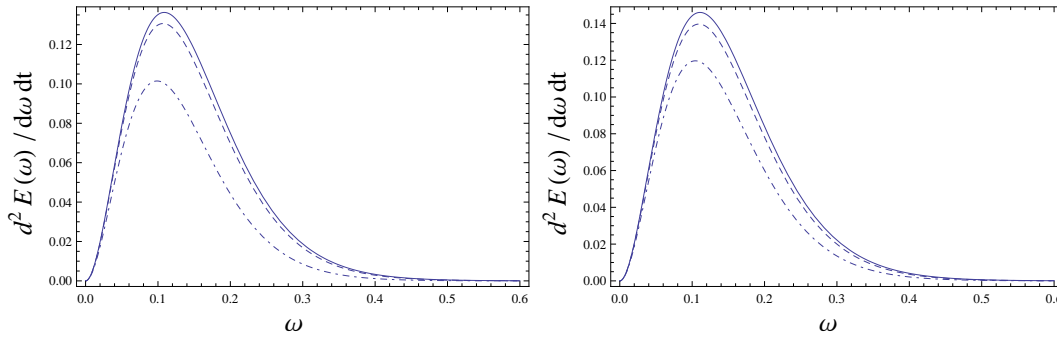


**Fig. 7** Dependence of the energy emission from the frequency for the different values of spin parameter  $a$ :  $a/M = 0.1$  (solid line),  $a/M = 0.3$  (dashed line),  $a/M = a_{ext}/M = 3\sqrt{3}/16$  (dot-dashed line). Left panel is for black hole in the Gauss-Bonnet and right panel is for 4D black hole in the Kerr space-time [38].

black hole as [39]

$$\alpha = \lim_{r_0 \rightarrow \infty} \left( -r_0^2 \sin \theta_0 \frac{d\phi}{dr} \right), \quad (25)$$

$$\beta = \lim_{r_0 \rightarrow \infty} r_0^2 \frac{d\theta}{dr}, \quad (26)$$

with  $r_0 \rightarrow \infty$ ,  $\theta_0$  is the inclination angle between the line of sight of the far observer and the axis of rotation of the black hole [40], also see [41].

Note here that a silhouette of the black hole is observed in 3-D space and here we would like to check the influence of the extra dimensions to the shape of the black hole shadow.

With the help of the expressions for the impact parameters derived in the Sec. 3 and the equations of motion obtained from the Hamilton-Jacobi equation (7), one can get  $d\phi/dr$  and  $d\theta/dr$ , and insert them into the equations (25) and (26) in order to get the explicit expressions for the celestial coordinates as

$$\alpha = -\xi \csc \theta_0, \quad (27)$$

$$\beta = \pm \sqrt{\eta + a^2 \cos^2 \theta_0 - \xi \cot^2 \theta_0}. \quad (28)$$

We will concentrate here on the special case when the inclination angle  $\theta_0 = \pi/2$  is similar to that for

four dimensional Kerr space-time (see e.g. [42,43,44, 36]). Then for the pure GB 6-D rotating black hole we have

$$\alpha = -\xi, \quad (29)$$

$$\beta = \pm \sqrt{\eta}. \quad (30)$$

To get boundary of the black hole shadow one can plot dependence of the coordinate  $\beta$  from the coordinate  $\alpha$ , see e.g. [41]. In Fig. 5, we compare shadow of six dimensional black hole in Gauss-Bonnet gravity with one of four dimensional Kerr black hole, which are shown for the different values of the rotation parameter  $a$ . The contours of the shadows of the Gauss-Bonnet black hole for the spin parameters  $a = 0$ ,  $a = a_{ext}/2$ , and  $a = a_{ext}$  are shown in Fig. 5. One can easily see, photon sphere is decreased with the increase of spin of the black hole in Gauss-Bonnet gravity. This behavior is exactly the same as in the Kerr space-time.

The observable parameters as distortion parameter  $\delta_s$  and radius of the shadow  $R_s$  can be computed numerically using either the expressions (29) and (30) or Fig. 5. Distortion parameter  $\delta_s = \Delta x/R_s$  [41,36], where  $\Delta x$  is deviation parameter which is distance between edge point of full circle and edge point of shadow [41]. Con-

sequently if rotation parameter is equal to zero  $a = 0$  then  $\Delta x$  must vanish. On the other hand, if we consider rotating black hole,  $\Delta x$  is nonzero and consequently  $\delta_s$  depends on spin of black hole. In Fig. 6, the observables  $R_s$  and  $\delta_s$  as functions of the rotation parameter of the black hole are shown when the inclination angle  $\theta_0 = \pi/2$ . From these plots one may conclude that with the increase of spin parameter  $a$  of the black hole in Gauss-Bonnet gravity shape of shadow is decreasing which is similar to the Kerr black hole case. The increase of  $\delta_s$  with the increase of rotation parameter  $a$  corresponds to deviation of the shape of shadow from circle.

## 5 Energetics

### 5.1 Emission energy of 6D rotating black hole

As the next step we plan to calculate energy emission from rotating black hole in higher dimensional Gauss-Bonnet gravity as [38]

$$\frac{d^2 E(\omega)}{d\omega dt} = \frac{2\pi^3 R_s^2}{e^{\omega/T} - 1} \omega^3, \quad (31)$$

where  $\omega$  is the frequency of the emission,  $T = (r_+^2 - 3a^2) / (8\pi r_+(r_+^2 + a^2))$  is the Hawking temperature for the Gauss-Bonnet black hole (for comparison,  $T = (r_+^2 - a^2) / (4\pi r_+(r_+^2 + a^2))$  is the Hawking temperature of the Kerr black hole [38]), which can be computed from this expression  $T = k/2\pi$ ,  $k$  is surface gravity.  $R_s$  is radius of shadow which is shown in Fig. 6 for the second order Lovelock space-time [38].

The comparison of the energy emission of rotating black hole in Gauss-Bonnet and Kerr space-time for the different values of spin parameters  $a$ :  $a = 0.1$  (solid line),  $a = 0.2$  (dashed line),  $a = 0.3$  (dot-dashed line) is represented in Fig. 7. The rate of energy emission decreases as the rotation parameter increases. The emission is more intense for the Kerr black hole as compared to GB one.

### 5.2 Particle acceleration through BSW effect

Here first we define the energy  $E_{\text{cm}}$  in the center of mass of system of two colliding particles with energy at infinity  $E_1$  and  $E_2$  in the gravitational field described by spacetime metric (3) as

$$E_{\text{cm}}^2 = p_{(\text{tot})}^\alpha p_{(\text{tot})\alpha}, \quad (32)$$

where  $p_{(\text{tot})}^\alpha = p_{(1)}^\alpha + p_{(2)}^\alpha$  is the total momenta of particles 1 and 2 with the mass  $m_1, m_2$ , respectively. We assume that two particles with equal mass ( $m_1 = m_2 =$

$m_0$ ) have the energy at infinity  $E_1 = E_2 \simeq 1$ , and consequently

$$E_{\text{cm}} = m_0 \sqrt{2} \sqrt{1 - g_{\alpha\beta} v_{(1)}^\alpha v_{(2)}^\beta}. \quad (33)$$

Now using the equations (19)–(21) we derive expression for the center-of-mass energy of particles in collision in the vicinity of the Gauss-Bonnet black hole as

$$\begin{aligned} \frac{E_{\text{c.m.}}^2}{2m^2} &= \frac{1}{\sqrt{r}(a^2 - r^{3/2} + r^2)} \\ &\times \left( a^2(1 + 2\sqrt{r}) - r^2 - a(l_1 + l_2) \right. \\ &\quad \left. - l_1 l_2 (\sqrt{r} - 1) + 2r^{5/2} - r^{5/2} \right. \\ &\quad \times \sqrt{a^2 - 2al_1 - l_1^2(\sqrt{r} - 1) + r^2} \\ &\quad \left. \times \sqrt{a^2 - 2al_2 - l_2^2(\sqrt{r} - 1) + r^2} \right), \quad (34) \end{aligned}$$

where we put  $M = 1$  and  $l_1 = L_1/m_1, l_2 = L_2/m_2$ .

For the extremal rotating Gauss-Bonnet black hole when  $a = 3\sqrt{3}/16$  the center of mass energy at the horizon has the following limit

$$\frac{E_{\text{c.m.}}^2}{2m^2}(r \rightarrow r_+) = \sqrt{\left(\frac{3\sqrt{3} - 4l_1}{3\sqrt{3} - 4l_2}\right)^3 + \left(\frac{3\sqrt{3} - 4l_2}{3\sqrt{3} - 4l_1}\right)^3} \quad (35)$$

Now we study the maximal energy which can be extracted through the BSW process [17] discussed in the Introduction from rotating Gauss-Bonnet black hole. For this purpose, first we need to study the energy of the test particle moving on the innermost stable circular orbit. Then we define the coefficient of total amount of released energy of the test particle on shifting from its stable circular orbit with the radius  $r_c$  to the ISCO with the radius  $r_{\text{ISCO}}$ . The energy release efficiency coefficient can be given as

$$\eta = 100 \times \frac{E(r_c) - E(r_{\text{ISCO}})}{E(r_c)}. \quad (36)$$

The radial dependence of the efficiency coefficient  $\eta$  for the different values of the rotation parameter  $a$  is shown in Fig. 8. The maximal energy extraction is for extremal black hole for which  $r_{\text{ISCO}} = r_h$  and so we obtain the maximal limit as  $\eta \simeq 55.28\%$ .

### 5.3 Penrose process

The existence of an ergosphere around the rotating black hole, where negative energy states for the particles moving along the timelike or null trajectory present, gives us opportunity to consider the energy extraction from the rotating black hole through Penrose process. Assume a small particle  $A$  falls down into the ergosphere of the black hole from far outside. In the vicinity of the



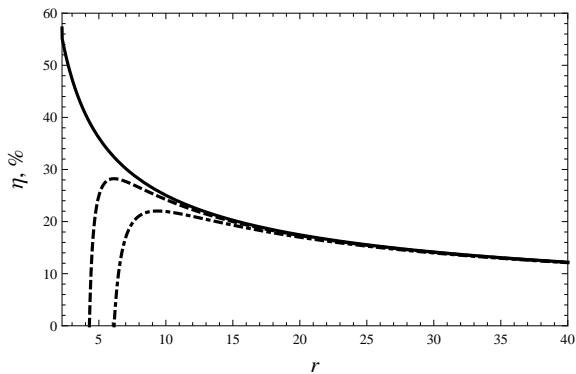


**Fig. 8** The radial dependence of energy extraction efficiency for the different values of the rotational parameter:  $a = 0.1$  (dot-dashed line),  $a = .3$  (dashed line), and  $a = 3\sqrt{3}/16$  (solid line).

event horizon it splits into two fragments,  $B$  and  $C$ . If particle  $B$  with the negative energy with respect to infinity falls into the central black hole then the emergent particle  $C$  has the energy exceeding the energy of the incident particle  $A$ .

$$\alpha E^2 - 2\beta E + \gamma + \frac{\Sigma}{\Delta}(p^r)^2 + \Sigma(p^\theta)^2 + r^2 \cos^2 \theta (p^\psi)^2 + m^2 = 0, \quad (37)$$

where we have used the following notations

$$\alpha = \Sigma (a^4 + 2a^2 r^2 + r^4 - a^2 \Delta \sin^2 \theta) \Gamma^{-1}, \quad (38)$$

$$\beta = -2M^{1/2} a r^{3/2} L \Sigma \Gamma^{-1}, \quad (39)$$

$$\gamma = \frac{L^2 \Sigma (a^2 \sin^2 \theta - \Delta)}{\Gamma \sin^2 \theta} + \frac{W^2}{r^2 \cos^2 \theta \sin^2 \psi}, \quad (40)$$

$$\Gamma = a^2 [(a^2 + r^2)^2 + \Delta^2 - Mr^3] \sin^2 \theta - \Delta (a^2 + r^2)^2 - a^4 \Delta \sin^4 \theta. \quad (41)$$

As the particle falls inside the event horizon the change of the mass of central rotating black hole defined as  $\delta M = E$ . In principle one can increase the mass of the black hole increasing the number of the infalling test particles with positive energy. The minimum value of the central black hole mass  $\delta M$  is achieved for condition when  $m = 0$ ,  $p^\theta = 0$ ,  $p^\psi = 0$ , and  $p^r = 0$ . Then one can get the expression for the minimum energy:

$$E_{\min} = \Omega(r_+) \mathcal{L}, \quad (42)$$

where we have used the notation

$$\Omega(r_+) = - \left. \frac{g_{03}}{g_{33}} \right|_{r=r_+} = \frac{2aM^{1/2} r_+^{3/2}}{a^2 + r_+^2}$$

using the values of the mass of the particle and momenta for the minimum condition.

Next we discuss the energy extraction efficiency from Gauss-Bonnet black hole through Penrose process. As in the case of BSW process we introduce the coefficient of efficiency of the Penrose process as

$$\eta_P = \frac{E_C - E_B}{E_A} \times 100, \quad (43)$$

where  $E_A$  is the energy of the incident particle and  $E_C$  is that of the emergent outgoing one. Using the energy conservation law for the particles  $A$ ,  $B$  and  $C$  one can find the maximal value of  $\eta_P$  in the form

$$\eta_{P(max)} = \left[ (\sqrt{1 + g_{tt}} + 1) / 2 - 1 \right] \times 100. \quad (44)$$

Evaluating this expression near the event horizon of extreme rotating Gauss-Bonnet black hole one can find the maximal efficiency of the value of 25.8%. Note that the energy extraction efficiency for the Penrose process in the case of extreme rotating 4-D Kerr black hole was found to be 20.7% [45, 13].

## 6 Discussion

The elemental feature of pure Lovelock gravity is that gravitational dynamics in all odd and even dimensions is similar. That is why it is expected that physical processes and effects around a 6-dimensional rotating pure GB black hole would be similar to that of 4-dimensional Kerr black hole. It should however be admitted that the black hole metric we have considered has all the desired features of a rotating black hole but it is though not an exact solution of the pure Lovelock vacuum equation. It does however satisfy the equation in the leading order which is computed as follows. Since metric goes as  $r^{-1/2}$ , Riemann tensor will go as  $r^{-5/2}$ , and then GB Ricci tensor will go as  $r^{-5}$ . For the black hole metric (2), GB Ricci tensor in fact falls off as  $r^{-7}$ , two powers sharper. It could therefore be taken as a good model for describing a rotating pure GB black hole.

As gravitational potential is weaker than Einstein gravity, its effects are reflected as follows. The efficiency of Penrose process decreases and it is reduced to 7.74% (it is equal to is 29% for the 4-D Kerr black hole) while the opposite is effect on particle acceleration efficiency which is increased to 55.28% (it is equal to 46% for the 4-D Kerr black hole). The center-of-mass energy rapidly grows for a collision of particles falling from infinity into rotating GB black hole in the case when the circular orbits shift arbitrarily close to the horizon. The optical shadow of black hole also decreases as lesser number of photons get captured because of weakening of the field. All these results are in on the expected lines on physical grounds, and hence they provide strength to validity and viability of the spacetime metric used.

In other way, this study could be looked upon probing the metric in question for its in principle physical and astrophysical validity.

We had set out to study various physical properties of a pure GB rotating black hole and show that they are indeed similar to the rotating black hole in the usual four dimensional physical spacetime. All this is in line with the pure Lovelock gravity paradigm [29] in higher dimensions.

## Acknowledgments

The authors acknowledge the project Supporting Integration with the International Theoretical and Observational Research Network in Relativistic Astrophysics of Compact Objects, CZ.1.07/2.3.00/20.0071, supported by Operational Programme *Education for Competitiveness* funded by Structural Funds of the European Union. One of the authors (ZS) acknowledges the Albert Einstein Center for gravitation and astrophysics supported by the Czech Science Foundation No. 14-37086G. Warm hospitality that has facilitated this work to A.A., B.A. and N.D. by Faculty of Philosophy and Science, Silesian University in Opava (Czech Republic) and by the Goethe University, Frankfurt am Main, Germany is thankfully acknowledged. This research is supported in part by Projects No. F2-FA-F113, No. EF2-FA-0-12477, and No. F2-FA-F029 of the UzAS and by the ICTP through the OEA-PRJ-29 and the OEA-NET-76 projects and by the Volkswagen Stiftung (Grant No. 86 866). A.A. and B.A. acknowledge the TWAS associateship grant.

## References

1. Lovelock D 1971 *J. Math. Phys.* **12** 498–501
2. Dadhich N 2004 *ArXiv General Relativity and Quantum Cosmology e-prints (Preprint gr-qc/0405115)*
3. Dadhich N 2005 *ArXiv High Energy Physics - Theory e-prints (Preprint hep-th/0509126)*
4. Dadhich N 2011 *International Journal of Modern Physics D* **20** 2739–2747 (*Preprint* 1105.3396)
5. Bañados M, Teitelboim C and Zanelli J 1994 *Physical Review Letters* **72** 957–960 (*Preprint* gr-qc/9309026)
6. Dadhich N 2012 *ArXiv e-prints (Preprint* 1210.3022)
7. Dadhich N, Ghosh S G and Jhingan S 2012 *Physics Letters B* **711** 196–198 (*Preprint* 1202.4575)
8. Camanho X O and Dadhich N 2015 *ArXiv e-prints (Preprint* 1503.02889)
9. Penrose R 1969 *Riv. Nuovo Cimento* **1** 252
10. Wagh S M, Dhurandhar S V and Dadhich N 1985 *Astrophys J.* **290** 12–14
11. Wagh S M, Dhurandhar S V and Dadhich N 1986 *Astrophys J.* **301** 1018
12. Wagh S M, Dhurandhar S V and Dadhich N 1985 *in Quasars, eds G. Swarup and V. Kapahi (Proc. 4th IAU Symposium 119, Bangalore, 1985, Reidel, Dordrecht)*
13. Parthasarathy S, Wagh S M and Dadhich N 1986 *Astrophys. J.* **307** 38
14. Dadhich N 2012 *ArXiv e-prints (Preprint* 1210.1041)
15. Koide S and Baba T 2014 *Astrophys J.* **792** 88 (*Preprint* 1407.7088)
16. Blandford R D and Znajek R L 1977 *Mon. Not. Roy. Astron. Soc.* **179** 433–456
17. Bañados M, Silk J and West S M 2009 *Physical Review Letters* **103** 111102
18. Virbhadra K S and Ellis G F R 2000 *Phys. Rev. D* **62** 084003
19. Virbhadra K S 2009 *Phys. Rev. D* **79** 083004
20. Bozza V, de Luca F, Scarpetta G and Sereno M 2005 *Phys. Rev. D.* **72** 083003
21. Bambi C and Yoshida N 2010 *Classical and Quantum Gravity* **27** 205006 (*Preprint* 1004.3149)
22. Grenzebach A, Perlick V and Lämmerzahl C 2014 *Phys. Rev. D* **89** 124004 (*Preprint* 1403.5234)
23. Falcke H and Markoff S B 2013 *Class. Quantum Grav* **30** 244003
24. Abdujabbarov A A, Rezzolla L and Ahmedov B J 2015 *ArXiv e-prints (Preprint* 1503.09054)
25. Stuchlík Z and Schee J 2013 *Classical and Quantum Gravity* **30** 075012
26. Stuchlík Z and Schee J 2010 *Classical and Quantum Gravity* **27** 215017 (*Preprint* 1101.3569)
27. Dadhich N, Ghosh S G and Jhingan S 2013 *Phys. Rev. D* **88** 124040 (*Preprint* 1308.4770)
28. Dadhich N and Ghosh S G 2013 *ArXiv e-prints (Preprint* 1307.6166)
29. Dadhich N 2015 *ArXiv e-prints (Preprint* 1506.08764)
30. Hansen D and Yunes N 2013 *Phys. Rev. D* **88** 104020 (*Preprint* 1308.6631)
31. Dadhich N 2013 *General Relativity and Gravitation* **45** 2383–2388 (*Preprint* 1301.5314)
32. Frolov V P and Kubizňák D 2008 *Classical and Quantum Gravity* **25** 154005 (*Preprint* 0802.0322)
33. Frolov V and Stojković D 2003 *Phys. Rev. D* **68** 064011 (*Preprint* gr-qc/0301016)
34. Papnoi U, Atamurotov F, Ghosh S G and Ahmedov B 2014 *Phys. Rev. D* **90** 024073 (*Preprint* 1407.0834)
35. Hackmann E, Kagramanova V, Kunz J and Lämmerzahl C 2008 *Phys. Rev. D* **78** 124018 (*Preprint* 0812.2428)
36. Hioki K and Maeda K I 2009 *Phys. Rev. D* **80** 024042
37. Zakharov A F, Nucita A A, De Paolis F and Ingrosso G 2005 *New Astron. Rev.* **10** 479–489
38. Wei S W and Liu Y X 2013 *JCAP* **11** 063
39. Vázquez S E and Esteban E P 2004 *Nuovo Cim. B* **119** 489
40. Amarilla L and Eiroa E F 2012 *Phys. Rev. D* **85** 064019
41. Atamurotov F, Abdujabbarov A and Ahmedov B 2013 *Phys. Rev. D* **88** 064004
42. Stuchlík Z and Schee J 2012 *Classical and Quantum Gravity* **29** 065002
43. Amarilla L, Eiroa E F and Giribet G 2010 *Phys. Rev. D* **81** 124045
44. Amarilla L and Eiroa E F 2013 *Phys. Rev. D* **87** 044057
45. Chandrasekhar S 1998 *The mathematical theory of black holes* (New York: Oxford University Press.)